Eur. Phys. J. D **20**, 481–497 (2002)
DOI: 10.1140/epjd/e2002-00155-6

THE EUROPEAN PHYSICAL JOURNAL D

The role of enhanced aromatic π-electron donating aptitude of the tyrosyl sidechain with respect to that of phenylalanyl in intramolecular interactions

G.A. Chass[1,2,3,a], S. Lovas[1,b], R.F. Murphy[1,c], and I.G. Csizmadia[2,3,d]

[1] Department of Biomedical Sciences, School of Medicine Creighton University, 2500 California Plaza, Omaha, NE 68178, USA
[2] Global Institute Of Computational Molecular and Material Science @ Velocet, 210 Dundas St. W., Toronto, Ontario, Canada M5G 2E8
[3] Department of Chemistry, University of Toronto, Lash Miller Chemical Laboratories, 80 St. George St., Toronto, Ontario, Canada M5S 3H6

Received 1st February 2002 / Received in final form 28 May 2002
Published online 13 September 2002 –

Abstract. An exhaustive *ab initio* and DFT search for energetically stable conformers from the topologically possible set was undertaken on the N-acetyl-phenylalanyl-N-methylamide and N-acetyl-tyrosyl-N-methylamide systems. The geometries of all 81 phenylalanyl and 162 tyrosyl possible rotamers, described under the rules outlined by Multi-Dimensional Conformational Analysis (MDCA), were attempted at each of the RHF/3-21G, RHF/6-31G(d) and B3LYP/6-31G(d) levels of theory. A total of 32 and 66 stable conformational minima were found for the phenylalanyl and tyrosyl amino acid diamides, respectively, at the B3LYP/6-31G(d) level. From the tyrosyl set, 33 unique conformers emerge when the orientation of the A_i^3 dihedral angle (p-OH orientation) is disregarded. A total of 31 conformers were common to both sets and showed nearly identical geometries. The comparison of the optimized DFT geometries of the two systems showed near by perfect linear fits with R^2 values of 0.9997, 0.9994, 0.9997, and 0.9996 for the ϕ_i, ψ_i, A_i^1, and A_i^2 dihedral angles, respectively. Relative energies of the matching 31 conformers also fitted to a linear plot with an R^2 value of 0.9985. The geometric centroid of the aromatic ring in the sidechain of both systems was found to be within 4.1 Å of the H and O atoms of the peptide groups, in 21 and 2 of the conformers, respectively. None of the non-matching conformers showed any such interaction distance $\leq$4.1 Å.

PACS. 31.15.Ar Ab initio calculations – 31.50.Bc Potential energy surfaces for ground electronic states – 33.15.Bh General molecular conformation and symmetry; stereochemistry

1 Introduction

The role of aromatic substituents, such as electron withdrawing and electron donating groups, in making the π-electron density of an aromatic ring tighter or looser, has been known since the early work of Hammett during the first half of the 20th century [1].

Nitration of phenol occurs at approximately 285 000 times the rate of that of benzene, indicating that the hydroxyl substituent lowers the energy of activation by about 7.3 kcal mol^{-1}; using 5.93 and 0.92 for ρ and σ, respectively [2]:

$$k_{\mathrm{OH}}/k_{\mathrm{H}} = 10^{\rho\sigma+} \approx 2.85 \times 10^5,$$
$$\Delta E_a = 5.4556RT/\log e = 7.34 \text{ kcal mol}^{-1}.$$

This activation barrier may in part be due to the enhanced π-electron donating aptitude of the aromatic ring upon hydroxyl substitution.

The π-electron donating aptitude is enhanced by hydroxyl substitution even in weak interactions between the aromatic ring and the amide hydrogen (Ar-HN) Scheme 1.

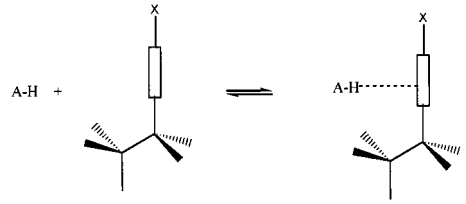

Scheme 1.

The rectangular open box in Scheme 1 represents the aromatic ring, where X = H, OH.

[a] e-mail: gchass@fixy.org
[b] e-mail: slovas@bif1.creighton.edu (author for correspondance)
[c] e-mail: barrym@creighton.edu
[d] e-mail: icsizmad@fixy.org

When phenylalanyl and tyrosyl residues occupy position i in a peptide sequence, they have two relatively acidic neighbouring peptide bonds. One is associated with position (i) (left side N–H) while the other one is associated with position $i+1$ (right side N–H), shown in Scheme 2. The thicker bold line joining the N(i) and N$(i+1)$ represents the bonds between the backbone atoms.

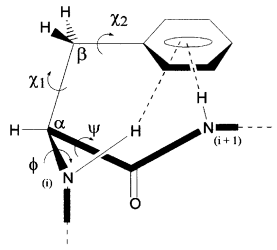

Scheme 2.

In protein secondary structures, such as in α-helices, most of the Hs of the amide bond are tied up in holding the structure together. Consequently, they may be less available for interaction with any aromatic rings. Although backbone conformation appears to play no role in mediating the formation of such aromatic amide interactions [4], the possibility can be still examined further. At the two edges of a parallel or anti-parallel β-sheet, half the amide hydrogens are tied up to hold the structure together but the others are free to form an interaction with an aromatic side chain. These relatively free protons are in either the i or the $i+1$ position. Other conformations also have either the ith or the $(i+1)$st N–H group blocked by backbone/backbone intramolecular H-bonds. For example in the γ_{L} (C_7) backbone conformation only the ith N–H group, while in the β_{L} (C_5) backbone conformation only the $(i+1)$st N–H group, is available for H-bond donation to the aromatic ring acceptor (Scheme 3).

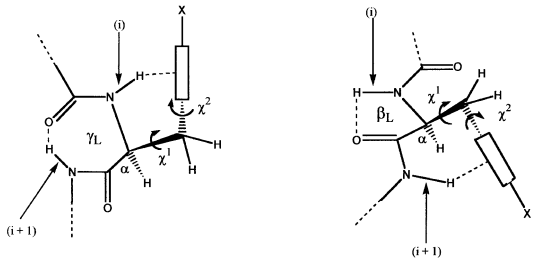

Scheme 3.

By contrast other backbone conformations may allow both the ith and the $(i+1)$st N–H groups to be available for interaction with an aromatic side-chain. Such intramolecular interactions can occur only at restricted combinations of values of the four key-dihedral angles (ϕ_i, ψ_i, χ_i^1, and χ_i^2). Consequently, a full conformational analysis is key to defining aromatic side-chain/backbone-amide interaction. This analysis is best conducted within the rules outlined in Multi-Dimensional Conformational Analysis (MDCA) [5], which states the potential for 9 backbone conformational minima, as well as for 3 for each saturated C–C bond along the sidechain. Non-saturated bonds along the side chain should have only two conformational minima. Phenyl hydroxyl groups and carboxylic acid groups may also have only two minima.

An attempt has been made to model the free phenylalanine and tyrosine amino acids [6]. These models of course exclude the interactions, whether steric or stabilizing, a side chain would have when its parent residue is in a peptide backbone. The free amino and acidic carboxyl groups may even help to stabilize conformers which would otherwise be excluded from a stable self-consistent model peptide set. Alternatively, free amino group hydrogens may be involved in the much stronger amine-carboxyl and amine-carbonyl H-bonds. The amine-carbonyl oxygen H-bonding in free amino acids would be more pronounced than in the corresponding amide to carbonyl H-bonding in peptides. Therefore they are not as readily available for the Ar–HN interactions. This structure would also allow for carboxyl hydrogen H-bonding with the carbonyl oxygen, which does not exist in polypeptides.

Ar–HN interactions are not the only ones observed along the polypeptide backbone. Other aromatic interactions with the atoms of the peptide group may also occur. All atoms of the peptide group acting together as a whole have a potential for interaction as π-donating or π-accepting centers, forming π-π type interactions. Model systems of this type of interaction have been studied in great detail to uncover and characterize all possible types [7–12] although the limited models used are not fully conclusive for polypeptides. All potential conformers for model peptides must therefore be located and examined to reveal the character of the interaction and which atoms are involved.

Clearly an amino acid diamide, as model peptide, will only allow for examination of the aromatic side chain to backbone interactions with position i and position $i+1$. However, these interactions must be further understood to complement the growing data on aromatic interactions with non-neighbouring positions $i \pm 2$ and $i \pm 3$ [13–16]. With a complete data set, the contribution of each these interactions can be characterized for their strengths and frequency of occurrence.

Construction of a topologically complete set of amino acid diamide conformers of the tyrosyl and phenylalanyl residues may reveal the actual number of stable minima falling within the selected thresholds of convergence, which emerge from the gas-phase, zero kelvin computations. Indeed solvation may provide stabilizing interactions and H-bonding that could allow some of the conformers that would otherwise be disallowed to exist within these thresholds. However, the number should be relatively small, as has been shown [17] to be the case, with each solvation-allowed conformer subject to their own of questions of validity. Results could be misleading unless a super-molecular approach is undertaken to model correctly the solvating particles. Although it is rarely practiced at the present time, at least one primary layer of

solvating molecules must also be explicitly defined, prior to immersing the molecular structure in an infinite dielectric medium.

2 Method

2.1 Construction of peptide modules (single amino acid diamides)

Segments or components of a peptide chain are consecutively numbered in their entireties. This modular approach allows quick additions, removals, rearrangements or substitutions of modules without having to redefine any other. Protecting groups of constituent amino acids are also numbered completely, prior to progressing to the next module. The numbering begins at the N-terminus and progresses to the C-terminus. The methodology follows the extensive set of rules outlined in works detailing the standardization of peptide computations [18].

Atoms of the peptide modules are numbered identically as far as the C_β (H in the case of glycine). In Figure 1, z is the number of atoms from the N-acetyl-end through the amino acid in the sequence, *i.e.* $z_{\mathrm{Gly}} = 13$, $z_{\mathrm{Ala}} = 16$, $z_{\mathrm{Val}} = 24$. Dihedral angle χ_i^1 (C_{14}–C_{13}–$C_{\alpha 8}$–N_7) represents the first side chain dihedral of the ith amino acid residue; and subsequent sidechain dihedrals increasing with superscript indices. The atoms of an amino acid are always numbered in the order N_7, C_8 (*i.e.* C_α), C_9, O_{10}, H_{11}, H_{12} and $C_{\beta 13}$ (H_{13} in the case of glycine).

By IUPAC definition, the following backbone dihedral angles (D) can be numerically depicted [19–27] as follows:

N – Protective

$$\begin{cases} \psi_{i-1} = (7,3,2,1) \equiv (1,2,3,7) & \longrightarrow D_7 \\ \omega_{i-1} = (8,7,3,2) \equiv (2,3,7,8) & \longrightarrow D_8 \end{cases}$$

Peptide – Residue

$$\begin{cases} \phi_i = (9,8,7,3) \equiv (3,7,8,9) & \longrightarrow D_9 \\ \psi_i = (z+1,9,8,7) \equiv (7,8,9,z+1) & \longrightarrow D_{z+1} \end{cases}$$

Peptide – Residue side chain

$$\begin{cases} \chi_i^1 = (14,13,8,9) \equiv (7,8,13,14) & \longrightarrow D_{14} \\ \chi_i^2 = (15,14,13,8) \equiv (8,13,14,15) & \longrightarrow D_{15} \\ \chi_i^3 = (25,24,17,16) \equiv (16,17,24,25) & \longrightarrow D_{25}. \end{cases}$$

C – Protective

$$\begin{cases} \omega_i = (z+2,z+1,9,8) \equiv (8,9,z+1,z+2) \\ \qquad\qquad\qquad\qquad\qquad\qquad \longrightarrow D_{z+2} \\ \phi_{i+1} = (z+3,z+2,z+1,9) \equiv (9,z+1,z+2,z+3) \\ \qquad\qquad\qquad\qquad\qquad\qquad \longrightarrow D_{z+3} \end{cases}$$

The side chain dihedral angles, χ_i^j are defined by IUPAC as the side chain to central backbone "heavy atom" spatial orientation relative to the peptide backbone. Thus, the atomic numbering and resultant dihedral numeric definitions progress along the side chain backbone, towards, and into the peptide backbone. For the phenylalanyl residue (Fig. 2) $z_{\mathrm{Phe}} = 6+20 = 26$, where 6 is the number of atoms in the acetyl group and 20 is the number of atoms in the residue. Similarly, in the tyrosyl group $z_{\mathrm{Tyr}} = 6+21 = 27$, where 6 is the number of atoms in the acetyl group and 21 is the number of atoms in the tyrosyl residue. These z-values may then be used to define the generalized dihedral angles listed above.

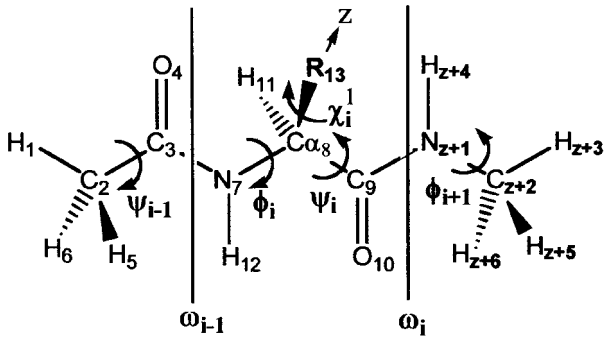

Figure 1. General numeric definition using standardized modular numbering system of atomic nuclei for each module of an amino acid diamide. z is the atomic center count reached after numbering the first two modules.

2.2 Molecular computations

An initial model peptide structure is first preoptimized with the AM1 semiempirical method. This is followed by the Hartree Fock *ab initio* level of computations using the 3-21G basis set, for construction and optimization of the topologically possible set of conformers predicted by MDCA. Geometry refinement is attained using the augmented split-valence 6-31G(d) basis set. In the final stage, electron correlation is induced at B3LYP/6-31G(d) level of theory. The Gaussian 98 program [28] was used for all molecular computations.

Convergence criteria of 3.0×10^{-4}, 4.5×10^{-4}, 1.2×10^{-3}, 1.8×10^{-3} are used for the gradients of the root mean square (RMS) force, maximum force, RMS displacement and maximum displacement vectors, respectively.

MDCA is used to generate the first input files for the tyrosine peptides. Ethyl benzene and *para*-hydroxy (*p*-OH) ethyl benzene geometry optimizations and scans were also prepared and computed in this manner.

The calculations for the tyrosyl residue are first completed and the resultant geometries used for the phenylalanyl calculations, at each matching level of theory. For example, the *p*-OH group in the input file is replaced by a H and the geometries are re-optimized. The computations are relatively quick to converge in most cases and when not so, are indicative of the coupling of the *p*-OH group to the overall geometry.

The MDCA methodology allows any one of the three rotamers, *gauche*$^+$ (g^+), *anti* (a) and *gauche*$^-$ (g^-), to exist along each torsional mode of ϕ_i, ψ_i, χ_i^1 and χ_i^2. The rotational potential of χ_i^3 is best approximated as having existing only 2 rotamers, *syn* (s) and a. The number of possible rotamers for each torsional mode is shown in Scheme 4 with the resultant number of topologically possible conformers also provided. Clearly the phenylalanyl

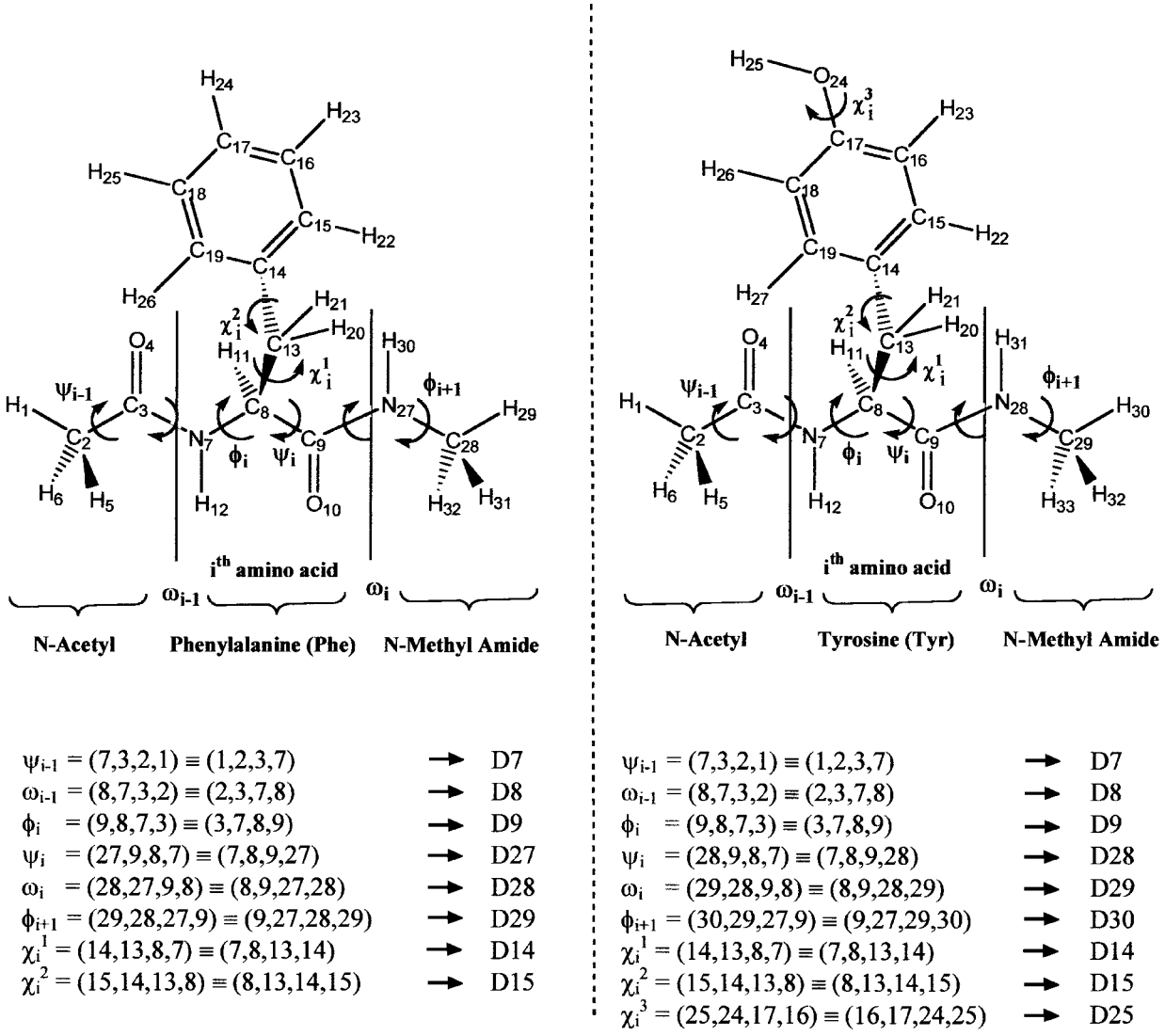

Figure 2. Complete numeric definitions using standardized modular numbering system of all atomic nuclei for N-acetyl-phenylalanyl-N-methylamide (left) and N-acetyl-tyrosyl-N-methylamide (right).

	ϕ_i		ψ_i		χ_i^1		χ_i^2		χ_i^3	
Phe	3	x	3	x	3	x	3			= 81 conformers
Tyr	3	x	3	x	3	x	3	x	2	= 162 conformers

Scheme 4.

residue *para*-H has no substantial χ_i^3 rotational potential. All conformers were constructed through numerical manipulation of their structural variables and their geometries were subsequently optimized through all 3 levels of theory in the above order. The input for each conformer made use of the output geometry of the previous level of theory, to formulate the geometry for the next higher level. Definition of any conformer that did not satisfy the convergence thresholds was re-computed at a geometry closer to the ideal formulated in MDCA, for that location on the hypersurface. For example, if a pre-optimized input from a geometry resulting from a lower level of theory were to provide a dihedral angle value outside the expected range (Tab. 1), resulting in a disappearance of a conformer, the implicated variable would then be reset to its ideal value for re-computation.

As examples, the structural properties of the three backbone conformers $\beta_{\rm L}$ (C_5), $\gamma_{\rm L}$ (C_7) and $\alpha_{\rm L}$, all with fully extended side chains, are given in their ideal states in Table 1. The dihedral numbers corresponding to the numbered structures in Figure 2, are shown.

Conformers persistently falling outside of the expected ranges are optimized with restrained dihedral angles (ϕ_i, ψ_i, χ_i^1 and χ_i^2), with the results being used to re-compute the conformer with these angles relaxed.

The computations of the $\chi_i^3 = a$ conformers of the tyrosyl structures were optimized prior to and of the $\chi_i^3 = s$ conformers. Calculations of the latter made use of the

Table 1. Examples of ideal MDCA values for dihedral angles in degrees for N-acetyl-phenylalanyl-N-methylamide and for N-acetyl-tyrosyl-N-methylamide.

	Conformer	ϕ_1 (D_9)	ψ_1 ($D_{27/28}$)**	χ_1^1 (D_{14})	χ_1^2 (D_{15})	χ_1^3 (D_{25})
Phe	β_L (C_5)	$\pm$180.0 (a)*	$\pm$180.0 (a)	$\pm$180.0 (a)	$\pm$180.0 (a)	-
	γ_L (C_7)	-60.0 (g^-)	$+60.0$ (g^+)	$\pm$180.0 (a)	$\pm$180.0 (a)	-
	α_L	-60.0 (g^-)	-60.0 (g^-)	$\pm$180.0 (a)	$\pm$180.0 (a)	-
Tyr	β_L (C_5)	$\pm$180.0 (a)	$\pm$180.0 (a)	$\pm$180.0 (a)	$\pm$180.0 (a)	$\pm$180.0 (a)
	γ_L (C_7)	-60.0 (g^-)	$+60.0$ (g^+)	$\pm$180.0 (a)	$\pm$180.0 (a)	$\pm$180.0 (a)
	α_L	-60.0 (g^-)	-60.0 (g^-)	$\pm$180.0 (a)	$\pm$180.0 (a)	$\pm$180.0 (a)

* The letter in parentheses represents the label for the area of conformational space that these ideal values fall within.
** Phenylalanine makes use of the D_{27} variable and tyrosine makes use of the D_{28} variable to define ψ_1.

optimized geometries of the $\chi_i^3 = a$ conformers. The dihedral angle χ_i^3 (D_{25}) was changed from 180.0 to 0.0 and these new geometries were re-optimized. Convergence was once again quick, as this extent of change in the χ_i^3 variable causes little perturbation of the full structure. Any calculation considerably longer than others, is considered likely to involve the χ_i^3 rotational potential in the overall stability. A simple numerical perturbation *in silico* may be indicative of a much larger and observable phenomenon *in vitro* and even *in vivo*.

It should be noted that the χ_i^2 and χ_i^3 rotations are coupled by the fact the $\chi_i^2, \chi_i^3 = g^+, a$ conformer is nearly the same as the $\chi_i^2, \chi_i^3 = g^-, s$ one. This relationship holds for the combinations of the two dihedral angles, as shown in Scheme 5, for all conformers of χ_i^1.

χ_i^2	χ_i^3		χ_i^2	χ_i^3
g^+	a	$\approx$	g^-	s
g^-	a	$\approx$	g^+	s

Scheme 5.

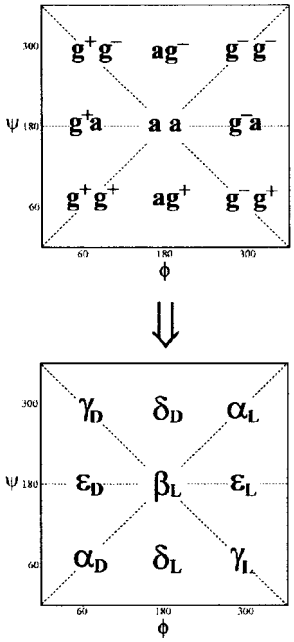

Figure 3. 2D-Ramachandran map providing the conformational assignments to the backbone dihedral angles (top) and their abbreviated nomenclature (bottom).

This work reports only the $\chi_i^3 = a$ conformers; works seeking to quantify the strengths of the Ar–HN and Ar$\cdots$H$_2$C interactions outlined above, may not be afforded the approximation outlined in Scheme 5.

When the geometric results of calculations progress from the lower (*e.g.* RHF/3-21G) to the higher level of theory [*e.g.* B3LYP/6-31G(d)] the Ramachandran PEHS becomes smoother. Consequently some relatively shallow minima, which are accommodated within the limits of MDCA at the lower level of theory, may no longer fall within the convergence thresholds at the augmented levels. Some of these conformers may be within the optimization thresholds when solvation is included.

2.3 Conformational nomenclature

Since an amino acid is principally a double rotor, involving two dihedral angles (ϕ and ψ), a total of $3\times3 = 9$ backbone conformers are expected. The conformational assignments (g^+g^+, ag^+, etc.) shown in Figure 3 (top) are a bit cumbersome to use. Very often some names are invented for sake of convenience. While names may be arbitrary, such as A, B, C, etc., more rational names might however be more appropriate. Such nomenclature is shown in Figure 3 (bottom).

The names (Fig. 3, bottom) are subscripted greek letters, originating from earlier nomenclature (involving α, β, and γ, etc. for α-helix, β-sheet, γ turn, etc.) apparent in Figure 4, while the L and D subscript originate from the observation that the L-amino acids favor L-subscripted conformations while D-amino acids favor D-subscripted conformations. The names also suggest that we are experiencing the combination of the chirality of the constitutional structure (R or S configuration) and the chirality origination from the conformational twist or folding.

Figure 5 summarizes the two "cuts" of the Ramachandran map used for analysis of the periodic behaviour of the ϕ and ψ dihedral angles. Figure 6 shows the symbolic pattern of the conformational potential energy surface (PES) for two full cycles of rotation ($-360° \rightarrow 0° \rightarrow +360°$). The four quadrants give the traditional cuts and the central square marked by broken lines, specifies a cut according to IUPAC convention (from $-180°$ to

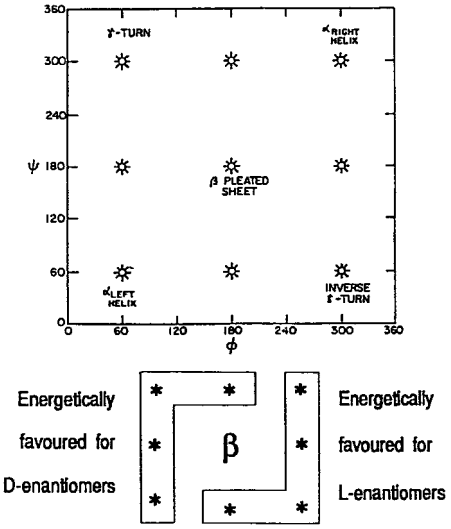

Figure 4. Logical reasoning for utilizing subscripted greek letters to reflect secondary structure attributed to each backbone conformer.

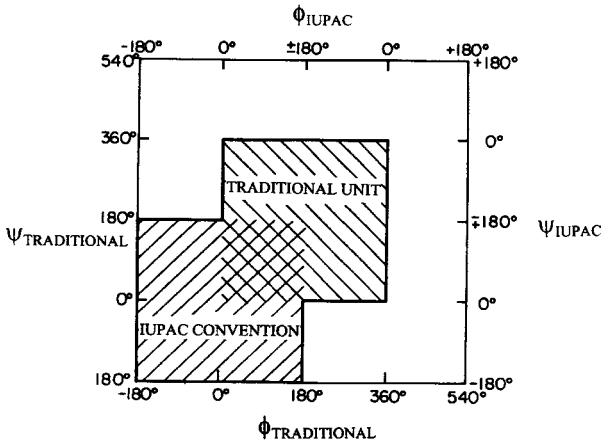

Figure 5. Partitioning of the peptide backbone conformational PES. The lower left hashed square shows the IUPAC cut ($-180° \rightarrow 0° \rightarrow +180°$). The central square shows the traditional cut ($0° \rightarrow 180° \rightarrow 360°$).

$+180°$), the negative sign corresponds to counter clockwise rotation while the positive sign denotes clockwise rotation. Sidechain dihedral angles make use of the g^+, a and g^- nomenclature for their conformational states. Extensive accounts and use of the methodology that this nomenclature is based upon can be found in the literature [29–34].

3 Results and discussion

Although a more complete basis set including diffuse and further polarization (beyond the d) functions is ideal, time and computational resources limited the work to the 6-31G(d) level of theory. As the two systems investigated do not carry any charge nor radical, the addition of diffuse functions may not significantly improve the results.

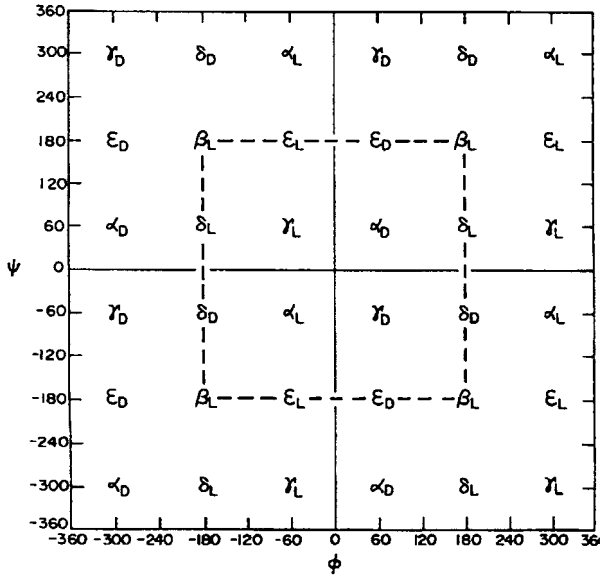

Figure 6. Representation of the peptide backbone conformational PES, with symbols showing the ideal locations of the topologically complete set of MDCA conformers.

The opportunity to explore a larger number of topologically possible conformers outweighed the alternative examination of a smaller number at a higher level of theory [*i.e.* 6-311++(2d, p)]. Quantification the relatively weak Ar$\cdots$HN interaction ($\sim$1–3 kcal mol^{-1}) may indeed benefit from such an improvement in the basis set.

Should the *p*-OH substitution in the benzene ring have no effect, then all observed stereochemical and energetic characteristics of the tyrosyl residue must be identical to those of the phenylalanyl residue. In some of the conformers, the effect of the *p*-OH hydroxyl substitution would cause only minor perturbation. However, noticeable differences may be seen in those conformations where the substituting OH group can affect, explicitly or implicitly, the molecular structure. Such effects should be related to some enhanced intramolecular interaction and could also be revealed by the extent of computation time, using optimized geometries of the tyrosyl residue to determine the phenylalanyl geometries. This is done simply by replacing the *p*-OH group with a H. Thus, the possible interactions which were considered were those between the aromatic side chain and the peptide group atoms and between the hydrogen of the phenolic –OH and the amide oxygen (*p*-OH$\cdots$O=C–NH), at positions i and $i+1$. The results show that the closest approach of this phenolic –OH hydrogen is approximately 6.0 Å and the *p*-OH$\cdots$O=C–NH is therefore not considered nor tabulated in this work.

The conventional identification of intra-backbone H-bonding is included, with the aromatic side chain centroid distances to the peptide group atoms in Tables 5 and 6, for the tyrosyl and phenyalanyl diamides, respectively.

3.1 Molecular conformations

Ethyl benzene and *p*-OH ethyl benzene have a global minimum at $\chi_2 = \pm 90°$ [35].

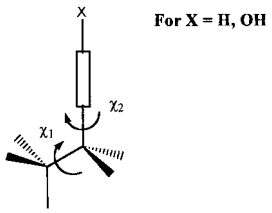

Scheme 6.

In the conformation depicted in Scheme 6, the benzene ring is perpendicular to the $H_3C–CH_2$ bond. Other higher energy minima ($\chi_2 = 0°$ and 180°) were shallow. Thus, only 6 side chain orientations are observed. If these 6 are coupled with the 9 possible backbone conformations, only $9 \times 6 = 54$ structures would need to be optimized. Conformers with $\chi_i^2 = 0°$ or $\chi_i^2 = 180°$ are also be observed. However, an attempt was made to locate all 9 possible side chain conformers, for each of the 9 backbone ones, in order to assure that all minima were identified. Only 6 minima emerged and were optimized, showing that each was identical. A slight perturbation of the χ_i^2 dihedral was observed in the *p*-OH substituted system.

The model side chain systems ethyl-benzene and *p*-OH-ethyl-benzene were scanned and shown as landscape and contour representations for both the RHF/3-21G and B3LYP/6-31G(d) levels of theory, afforded near identical PES (Fig. 7). The landscape representations reveal the "smoothening" of the Potential Energy Hyper Surfaces (PEHS) using the higher B3LYP level of theory compared with the lower RHF levels. In this region it can be seen that the depth of the two minima along the χ_i^2-axis is more pronounced for the RHF plots (indicated by arrows). The representations of the PEHSs were displayed such that the visual representations were identical, in order that the magnitude of this observed change was not a result of the viewing angles.

The lack of any detectable geometric difference between the two systems is evident. The *p*-OH substituted ethyl-benzene PEHS show the exact same conformational behaviour and location of minima as those of the non-substituted ethyl-benzene.

Tables 2 and 3 list the dihedral angles for the tyrosyl and phenylalanyl diamides respectively. All χ_i^2 orientations are in the vicinity of $\pm 90°$, (g^+ and g^-, respectively) and none are *s* ($\chi_i^2 = 0°$) or *a* ($\chi_i^2 = 180°$). Both systems converged to a near exact set of conformers with only one δ_L Tyr conformer ($\chi_i^1,\ \chi_i^2 = g^-,\ g^-$) shifting to an α_L conformer ($\chi_i^1,\ \chi_i^2 = g^+,\ g^+$).

Table 4 gives the differences between the corresponding torsional or dihedral angles (D)

$$\Delta D = D(\text{Tyr}) - D(\text{Phe}).$$

A ΔD larger by one standard deviation indicates that a tyrosyl dihedral angle is appreciably different from that of

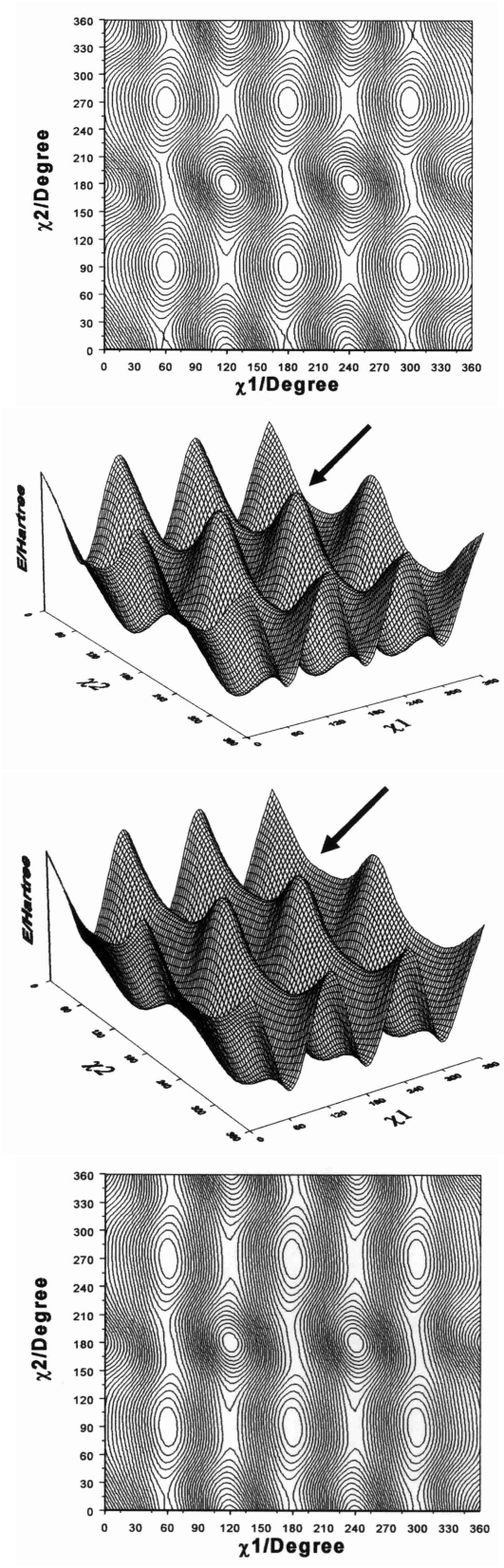

Figure 7. Contour and landscape (with arrows) representations of the 2D-Ramachandran PES for $E = f(\chi_1,\ \chi_2)$, for ethyl-benzene, computed at the RHF/3-21G (top 2) and the B3LYP/6-31G(d) (bottom 2) levels of theory.

Table 2. Dihedral angles in degrees, total energy and relative energy for N-acetyl-phenylalanyl-N-methylamide computed at the B3LYP/6-31G(d) level of theory.

Label	ϕ_i	ψ_i	χ_i^1	χ_i^2	ω_{i-1} (D_8)	ϕ_i ($D9$)	ψ_i (D_{27})	ω_i (D_{28})	χ_i^1 (D_{14})	χ_i^2 (D_{15})	χ_i^3 (D_{25})	E/Hartrees	Rel. E/kcal mol^{-1}
	a	a	g^+	g^+	175.33	−157.04	167.13	−178.91	59.93	90.74		−726.901313557	3.022
	a	a	g^+	a								N/F	
	a	a	g^+	g^-	174.84	−157.10	167.54	−178.71	59.89	−89.13		−726.901316987	3.020
	a	a	a	g^+	174.11	−158.33	170.46	176.78	−155.08	68.91		−726.904932002	0.751
β_{L}	a	a	a	a								N/F	
	a	a	a	g^-	174.72	−158.46	170.93	177.93	−155.18	−111.15		−726.904964815	0.731
	a	a	g^-	g^+	175.04	−124.21	145.53	178.47	−60.95	94.60		−726.899809260	3.966
	a	a	g^-	a								N/F	
	a	a	g^-	g^-	173.98	−124.02	144.93	178.73	−61.18	−84.78		−726.899842618	3.945
	g^-	g^+	g^+	g^+	−174.56	−82.75	58.73	178.80	42.33	77.21		−726.906129174	0.000
	g^-	g^+	g^+	a								N/F	
	g^-	g^+	g^+	g^-	−174.82	−82.71	58.83	178.95	42.21	−102.49		−726.906128778	0.000
	g^-	g^+	a	g^+	−177.01	−83.37	78.46	−174.16	−161.96	90.97		−726.904825171	0.818
γ_{L}	g^-	g^+	a	a								N/F	
	g^-	g^+	a	g^-	−178.37	−82.83	78.54	−174.30	−161.80	−87.51		−726.904843585	0.807
	g^-	g^+	g^-	g^+	−171.88	−84.64	71.74	−176.07	−54.81	110.11		−726.904496506	1.025
	g^-	g^+	g^-	a								N/F	
	g^-	g^+	g^-	g^-	−170.84	−84.11	72.64	−175.42	−54.50	−69.47		−726.904321097	1.135
	g^+	g^-	g^+	g^+	166.34	55.12	−22.88	−176.37	70.92	80.77		−726.894000858	7.611
	g^+	g^-	g^+	a								N/F	
	g^+	g^-	g^+	g^-									
	g^+	g^-	a	g^+	176.27	73.38	−66.58	176.58	−170.76	83.98		−726.899014652	4.464
γ_{D}	g^+	g^-	a	a								N/F	
	g^+	g^-	a	g^-	175.90	73.45	−66.63	176.51	−170.81	−95.83		−726.899010780	4.467
	g^+	g^-	g^-	g^+	169.94	75.18	−53.05	−177.86	−57.33	100.29		−726.901874086	2.670
	g^+	g^-	g^-	a								N/F	
	g^+	g^-	g^-	g^-	169.91	75.28	−53.26	−177.62	−57.33	−78.58		−726.901872664	2.671
	a	g^+	g^+	g^+	−170.08	−120.27	17.58	175.39	54.42	82.83		−726.902839138	2.065
	a	g^+	g^+	a								N/F	
	a	g^+	g^+	g^-	−170.20	−120.33	17.77	175.32	54.37	−95.96		−726.902838889	2.065
	a	g^+	a	g^+								N/F	
δ_{L}	a	g^+	a	a								N/F	
	a	g^+	a	g^-								N/F	
	a	g^+	g^-	g^+	−164.20	−119.25	14.43	175.08	−59.91	105.74		−726.899578383	4.111
	a	g^+	g^-	a								N/F	
	a	g^+	g^-	g^-	−163.95	−119.22	14.17	175.05	−59.80	−73.07		−726.899581573	4.109
	a	g^-	g^+	g^+	167.38	−174.54	−32.11	−171.84	58.29	91.45		−726.895260955	6.820
	a	g^-	g^+	a								N/F	
	a	g^-	g^+	g^-	170.05	−175.61	−33.00	−172.15	57.97	−89.06		−726.895237557	6.835
	a	g^-	a	g^+	171.84	−159.61	−53.91	−174.96	−173.24	77.72		−726.892303272	8.676
δ_{D}	a	g^-	a	a								N/F	
	a	g^-	a	g^-	172.06	−159.74	−53.50	−174.69	−173.63	−101.85		−726.892285384	8.687
	a	g^-	g^-	g^+								N/F	
	a	g^-	g^-	a								N/F	
	a	g^-	g^-	g^-								N/F	
	g^-	g^-	g^+	g^+								N/F	
	g^-	g^-	g^+	a								N/F	
	g^-	g^-	g^+	g^-								N/F	
	g^-	g^-	a	g^+								N/F	
α_{L}	g^-	g^-	a	a								N/F	
	g^-	g^-	a	g^-								N/F	
	g^-	g^-	g^-	g^+								N/F	
	g^-	g^-	g^-	a								N/F	
	g^-	g^-	g^-	g^-								N/F	
	g^+	g^+	g^+	g^+	161.96	48.94	44.39	−172.98	48.51	80.15		−726.891910860	8.922
	g^+	g^+	g^+	a								N/F	
	g^+	g^+	g^+	g^-									
	g^+	g^+	a	g^+	168.44	66.35	34.08	−177.06	−134.59	107.42		−726.893847142	7.707
α_{D}	g^+	g^+	a	a								N/F	
	g^+	g^+	a	g^-	168.39	66.47	33.74	−177.14	−134.22	−71.32		−726.893845635	7.708
	g^+	g^+	g^-	g^+	165.18	73.36	20.86	−177.96	−56.95	101.04		−726.897465686	5.436
	g^+	g^+	g^-	a								N/F	
	g^+	g^+	g^-	g^-	165.25	71.93	22.68	−177.18	−56.98	−77.64		−726.897458593	5.441
	g^-	a	g^+	g^+								N/F	
	g^-	a	g^+	a								N/F	
	g^-	a	g^+	g^-								N/F	
	g^-	a	a	g^+								N/F	
ε_{L}	g^-	a	a	a								N/F	
	g^-	a	a	g^-								N/F	
	g^-		g^-	g^+								N/F	
	g^-	a	g^-	a								N/F	
	g^-	a	g^-	g^-								N/F	
	g^+	a	g^+	g^+								N/F	
	g^+	a	g^+	a								N/F	
	g^+	a	g^+	g^-								N/F	
	g^+	a	a	g^+	−160.09	64.14	−164.04	−176.41	−157.22	59.96		−726.893880116	7.686
ε_{D}	g^+	a	a	a								N/F	
	g^+	a	a	g^-	−160.29	64.44	−164.56	−177.04	−156.63	−122.36		−726.893966603	7.632
	g^+	a	g^-	g^+								N/F	
	g^+	a	g^-	a								N/F	
	g^+	a	g^-	g^-								N/F	
	g^-	a	g^-	g^-								N/F	

Table 3. Dihedral angles in degrees, total energy and relative energy for N-acetyl-phenylalanyl-N-methylamide computed at the B3LYP/6-31G(d) level of theory.

Label	ϕ_1	ψ_1	χ_1	χ_1	ω_0 (D_8)	ϕ_1 (D_9)	ψ_1 (D_{28})	ω_1 (D_{29})	χ_1^1 (D_{14})	χ_1^2 (D_{15})	χ_1^3 (D_{25})	E/Hartrees	Rel. E/kcal mol^{-1}
	a	a	g^+	g^+	175.81	−156.37	167.86	−179.19	60.05	89.46	−179.96	−802.117367562	3.208
	a	a	g^+	a								N/F	
	a	a	g^+	g^-	173.85	−154.37	166.82	−179.16	59.82	−89.94	179.48	−802.117236991	3.290
	a	a	a	g^+	175.18	−158.649	169.13	176.83	−157.03	68.90	178.63	−802.120831742	1.043
β_L	a	a	a	a								N/F	
	a	a	a	g^-	174.65	−158.52	170.53	177.14	−154.44	−110.49	−178.88	−802.121197551	0.805
	a	a	g^-	g^+	176.49	−127.79	150.1	178.86	−57.54	98.96	−178.27	−802.115749174	4.224
	a	a	g^-	a								N/F	
	a	a	g^-	g^-	171.93	−119.45	144.09	178.68	−63.13	−88.14	179.22	−802.115679824	4.267
	g^-	g^+	g^+	g^+	−175.54	−81.10	56.22	177.83	43.48	76.76	178.45	−802.121991511	0.306
	g^-	g^+	g^+	a								N/F	
	g^-	g^+	g^+	g^-	−174.86	−81.57	56.40	177.80	43.72	−101.81	−178.93	−802.122479806	0.000
	g^-	g^+	a	g^+	−177.94	−82.86	78.12	−174.13	−162.58	92.87	−179.96	−802.121099136	0.866
γ_L	g^-	g^+	a	a								N/F	
	g^-	g^+	a	g^-	−178.41	−82.89	78.49	−174.24	−162.64	−86.25	179.84	−802.120793028	1.058
	g^-	g^+	g^-	g^+	−171.47	−84.66	71.96	−175.81	−54.73	109.08	179.47	−802.120402944	1.303
	g^-	g^+	g^-	a								N/F	
	g^-	g^+	g^-	g^-	−169.62	−84.52	72.9	−175.71	−53.58	−66.9	−178.94	−802.120128307	1.476
	g^+	g^-	g^+	g^+	170.04	54.60	−24.42	−175.8	72.22	81.19	−179.12	−802.110049332	7.800
	g^+	g^-	g^+	a								N/F	
	g^+	g^-	g^+	g^-	167.63	54.81	−21.65	−176.00	70.50	−100.43	179.43	−802.110188418	7.713
	g^+	g^-	a	g^+	176.33	73.41	−67.00	175.72	−170.52	85.24	−178.77	−802.115133370	4.610
γ_D	g^+	g^-	a	a								N/F	
	g^+	g^-	a	g^-	−179.57	70.87	−69.46	175.88	−173.00	−97.50	178.75	−802.114717276	4.871
	g^+	g^-	g^-	g^+	169.92	75.25	−53.49	−178.06	−57.32	99.14	178.76	−802.117790759	2.942
	g^+	g^-	g^-	a								N/F	
	g^+	g^-	g^-	g^-	170.14	75.48	−54.94	−178.61	−56.7	−78.13	−178.5	−802.117746263	2.970
	a	g^+	g^+	g^+	−170.38	−120.93	18.83	175.13	54.19	81.31	178.52	−802.118768168	2.329
	a	g^+	g^+	a								N/F	
	a	g^+	g^+	g^-	−169.73	−121.45	18.96	175.22	54.78	−96.38	−178.75	−802.119129892	2.102
	a	g^+	a	g^+								N/F	
δ_L	a	g^+	a	a								N/F	
	a	g^+	a	g^-								N/F	
	a	g^+	g^-	g^+	−163.47	−120.12	13.60	175.04	−59.23	105.50	179.98	−802.115701791	4.253
	a	g^+	g^-	a								N/F	
	a	g^+	g^-	g^-								N/F	
	a	g^-	g^+	g^+	168.26	−172.31	−34.47	−172.25	56.48	91.59	177.93	−802.111339732	6.991
	a	g^-	g^+	a								N/F	
	a	g^-	g^+	g^-	168.49	−173.76	−32.48	−171.78	58.61	−88.12	−177.85	−802.111225116	7.062
	a	g^-	a	g^+	171.99	−160.19	−52.56	−174.65	−172.66	78.35	−179.11	−802.108102670	9.022
δ_D	a	g^-	a	a								N/F	
	a	g^-	a	g^-	172.58	−158.69	−56.12	−174.7	−174.66	−102.87	179.02	−802.108411108	8.828
	a	g^-	g^-	g^+								N/F	
	a	g^-	g^-	a								N/F	
	a	g^-	g^-	g^-								N/F	
	g^-	g^-	g^+	g^+								N/F	
	g^-	g^-	g^+	a								N/F	
	g^-	g^-	g^+	g^-								N/F	
	g^-	g^-	a	g^+								N/F	
α_L	g^-	g^-	a	a								N/F	
	g^-	g^-	a	g^-								N/F	
	g^-	g^-	g^-	g^+								N/F	
	g^-	g^-	g^-	a								N/F	
	g^-	g^-	g^-	g^-	−165.65	−82.62	−13.43	176.32	−57.75	−68.47	−178.78	−802.114870584	4.775
	g^+	g^+	g^+	g^+	160.73	49.37	43.76	−173.06	49.70	78.39	179.61	−802.107606514	9.333
	g^+	g^+	g^+	a								N/F	
	g^+	g^+	g^+	g^-								N/F	
	g^+	g^+	a	g^+	167.73	64.32	37.23	−176.15	−139.67	100.78	179.38	−802.110080870	7.780
α_D	g^+	g^+	a	a								N/F	
	g^+	g^+	a	g^-	169.53	65.71	34.48	−176.47	−135.72	−72.05	−179.03	−802.109539378	8.120
	g^+	g^+	g^-	g^+	165.06	73.22	20.64	−177.60	−56.69	99.20	178.31	−802.113255603	5.788
	g^+	g^+	g^-	a								N/F	
	g^+	g^+	g^-	g^-	164.68	73.78	20.48	−178.08	−55.71	−77.22	181.98	−802.113265231	5.782
	g^-	a	g^+	g^+								N/F	
	g^-	a	g^+	a								N/F	
	g^-	a	g^+	g^-								N/F	
	g^-	a	a	g^+								N/F	
ε_L	g^-	a	a	a								N/F	
	g^-	a	a	g^-								N/F	
	g^-	a	g^-	g^+								N/F	
	g^-	a	g^-	a								N/F	
	g^-	a	g^-	g^-								N/F	
	g^+	a	g^+	g^+								N/F	
	g^+	a	g^+	a								N/F	
	g^+	a	g^+	g^-								N/F	
	g^+	a	a	g^+	−160.29	63.93	−163.66	−176.13	−158.06	59.68	−181.2	−802.109884154	7.904
ε_D	g^+	a	a								N/F		
	g^+	a	a	g^-	−165.83	68.96	−175.39	−176.79	−154.12	−124.29	−179.65	−802.109838527	7.933
	g^+	a	g^-	g^+								N/F	
	g^+	a	g^-	a								N/F	
	g^+	a	g^-	g^-								N/F	

Table 4. Difference in dihedral angles in degrees, total energy and relative energy for [Ac-Tyr-NH-Me] − [Ac-Phe-NH-Me], for matching conformers computed at the B3LYP/6-31G(d) level of theory.

Label	ϕ_i	ψ_i	χ_i^1	χ_i^2	ω_{i-1} (D_8)	ϕ_i (D_9)	ψ_i (Dz+1)	ω_i (Dz+2)	χ_i^1 (D_{14})	χ_i^2 (D_{15})	χ_i^3 (D_{25})	Rel. E/kcal mol^{-1}
	a	a	g^+	g^+	0.48	0.67	0.73	−0.28	0.12	−1.28		0.19
	a	a	g^+	a								
	a	a	g^+	g^-	−0.99	2.73	−0.72	−0.45	−0.07	−0.81		0.27
	a	a	a	g^+	1.07	−0.32	−1.33	0.05	−1.95	−0.01		0.29
β_L	a	a	a	a								
	a	a	a	g^-	−0.07	−0.06	−0.40	−0.79	0.74	0.66		0.07
	a	a	g^-	g^+	1.45	−3.58	4.57	0.39	3.41	4.36		0.26
	a	a	g^-	a								
	a	a	g^-	g^-	−2.05	4.57	−0.84	−0.05	−1.95	−3.36		0.32
	g^-	g^+	g^+	g^+	−0.98	1.65	−2.51	−0.97	1.15	−0.45		0.31
	g^-	g^+	g^+	a								
	g^-	g^+	g^+	g^-	−0.04	1.14	−2.43	−1.15	1.51	0.68		0.00
	g^-	g^+	a	g^+	−0.93	0.51	−0.34	0.03	−0.62	1.90		0.05
γ_L	g^-	g^+	a	a								
	g^-	g^+	a	g^-	−0.04	−0.06	−0.05	0.06	−0.84	1.26		0.25
	g^-	g^+	g^-	g^+	0.41	−0.02	0.22	0.26	0.08	−1.03		0.28
	g^-	g^+	g^-	a								
	g^-	g^+	g^-	g^-	1.22	−0.41	0.26	−0.29	0.92	2.57		0.34
	g^+	g^-	g^+	g^+	3.70	−0.52	−1.54	0.57	1.30	0.42		0.19
	g^+	g^-	g^+	a								
	g^+	g^-	g^+	g^-								
	g^+	g^-	a	g^+	0.06	0.03	−0.42	−0.86	0.24	1.26		0.15
γ_D	g^+	g^-	a	a								
	g^+	g^-	a	g^-	4.53	−2.58	−2.83	−0.63	−2.19	−1.67		0.40
	g^+	g^-	g^-	g^+	−0.02	0.07	−0.44	−0.20	0.01	−1.15		0.27
	g^+	g^-	g^-	a								
	g^+	g^-	g^-	g^-	0.23	0.20	−1.68	−0.99	0.63	0.45		0.30
	a	g^+	g^+	g^+	−0.3	−0.66	1.25	−0.26	−0.23	−1.52		0.26
	a	g^+	g^+	a								
	a	g^+	g^+	g^-	0.47	−1.12	1.19	−0.1	0.41	−0.42		0.04
	a	g^+	a	g^+								
δ_L	a	g^+	a	a								
	a	g^+	a	g^-								
	a	g^+	g^-	g^+	0.73	−0.87	−0.83	−0.04	0.68	−0.24		0.14
	a	g^+	g^-	a								
	a	g^+	g^-	g^-								
	a	g^-	g^+	g^+	0.88	2.23	−2.36	−0.41	−1.81	0.14		0.17
	a	g^-	g^+	a								
	a	g^-	g^+	g^-	−1.56	1.85	0.52	0.37	0.64	0.94		0.23
	a	g^-	a	g^+	0.15	−0.58	1.35	0.31	0.58	0.63		0.35
δ_D	a	g^-	a	a								
	a	g^-	a	g^-	0.52	1.05	−2.62	−0.01	−1.03	−1.02		0.14
	a	g^-	g^-	g^+								
	a	g^-	g^-	a								
	a	g^-	g^-	g^-								
	g^-	g^-	g^+	g^+								
	g^-	g^-	g^+	a								
	g^-	g^-	g^+	g^-								
	g^-	g^-	a	g^+								
α_L	g^-	g^-	a	a								
	g^-	g^-	a	g^-								
	g^-	g^-	g^-	g^+								
	g^-	g^-	g^-	a								
	g^-	g^-	g^-	g^-								
	g^+	g^+	g^+	g^+	−1.23	0.43	−0.63	−0.08	1.19	−1.76		0.41
	g^+	g^+	g^+	a								
	g^+	g^+	g^+	g^-								
	g^+	g^+	a	g^+	−0.71	−2.03	3.15	0.91	−5.08	−6.64		0.07
α_D	g^+	g^+	a	a								
	g^+	g^+	a	g^-	1.14	−0.76	0.74	0.67	−1.50	−0.73		0.41
	g^+	g^+	g^-	g^+	−0.12	−0.14	−0.22	0.36	0.26	−1.84		0.35
	g^+	g^+	g^-	a								
	g^+	g^+	g^-	g^-	−0.57	1.85	−2.20	−0.90	1.27	0.42		0.34
	g^-	a	g^+	g^+								
	g^-	a	g^+	a								
	g^-	a	g^+	g^-								
	g^-	a	a	g^+								
ε_L	g^-	a	a	a								
	g^-	a	a	g^-								
	g^-	a	g^-	g^+								
	g^-	a	g^-	a								
	g^-	a	g^-	g^-								
	g^+	a	g^+	g^+								
	g^+	a	g^+	a								
	g^+	a	g^+	g^-								
	g^+	a	a	g^+	−0.20	−0.21	0.38	0.28	−0.84	−0.28		0.22
ε_D	g^+	a	a	a								
	g^+	a	a	g^-	−5.54	4.52	−10.83	0.25	2.51	−1.93		0.30
	g^+	a	g^-	g^+								
	g^+	a	g^-	a								
	g^+	a	g^-	g^-								

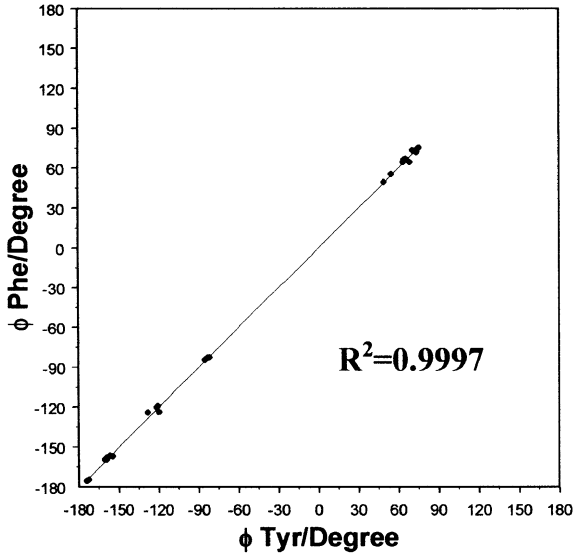

Figure 8. Linear fit plot of ϕ_{Tyr} against ϕ_{Phe}, for matching conformers, computed at the B3LYP/6-31G(d) level of theory.

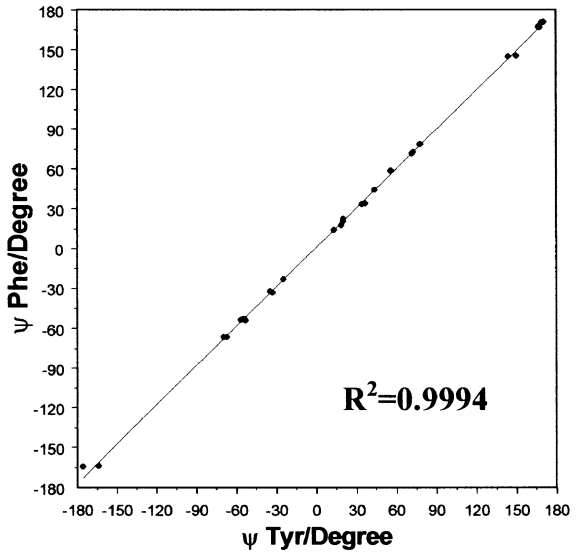

Figure 9. Linear fit plot of ψ_{Tyr} against ψ_{Phe}, for matching conformers, computed at the B3LYP/6-31G(d) level of theory.

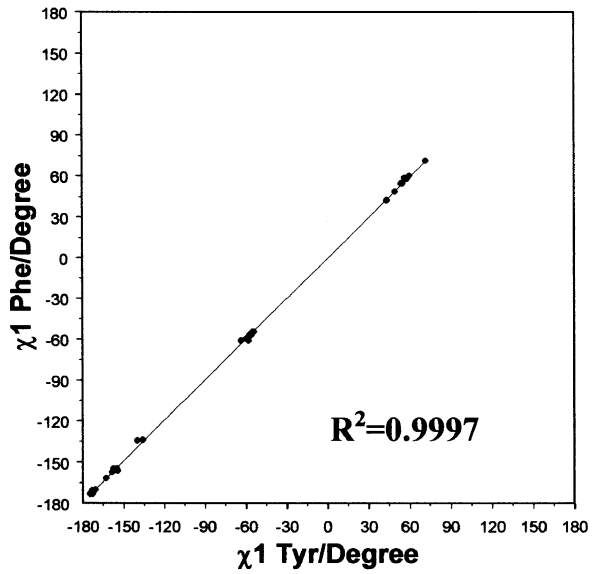

Figure 10. Linear fit plot of $\chi^1_{i\,\mathrm{Tyr}}$ against $\chi^1_{i\,\mathrm{Phe}}$, matching conformers, computed at the B3LYP/6-31G(d) level of theory.

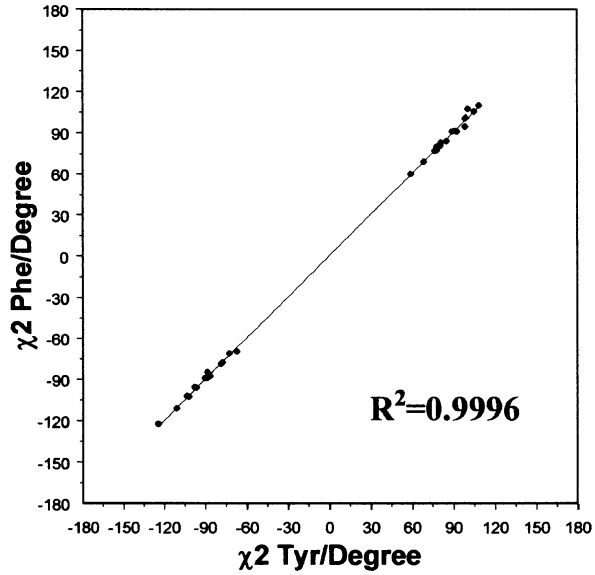

Figure 11. Linear fit plot of $\chi^1_{i\,\mathrm{Tyr}}$ against $\chi^1_{i\,\mathrm{Phe}}$, for matching conformers, computed at the B3LYP/6-31G(d) level of theory.

the corresponding phenylalanyl angle. This may be due to the influence of the aromatic *p*-OH in some intramolecular interaction.

D(Tyr) may be plotted against D(Phe) to determine which conformers deviate substantially from a 45° line. Figures 8, 9, 10 and 11 show such plots for ϕ_i, ψ_i, χ^1_i and χ^2_i respectively. It can be observed (from the spread of points in the corresponding figures) that ψ_i and χ^2_i are less ideal, in terms of population of their respective conformational space. These can be contrasted to the dihedral angles ϕ_i and χ^1_i, for example, which have most of the stable conformers populating ideal states predicted by MDCA. Figures 8 and 10 show such groupings of points at these topologically probable locals (g^+, a, g^-), for the ϕ_i and χ^1_i variables, respectively. Figures 9 and 11 show a spread of points, indicative of the quite flexible nature of each of the ψ_i and χ^2_i variables, respectively. Figure 8 also shows that the ϕ_i variable avoids any values $\geq$75° and $\leq$180°. Conformers with $\phi_i = a$ show a clear preference for the counter-clockwise rotation for the ϕ_i variable, which may be a attributed to the L-enantiomeric state of the peptide model. It is expected that the D-enantiomer would afford the inverse relationship. Specifically, conformers for the D-enantiomer with $\phi_i = a$ show a clear preference for the clockwise rotation for the ϕ_i variable.

Deviations from these ideal properties may be indicative of both important unexpected geometries as well as a need to refine the rules of MDCA for specific cases.

7.71 *g*+*g*- **7.61**	**4.87** *ag*- **4.47**	**2.97** *g-g*- **2.67**	**7.06** *g*+*g*- **6.84**	**8.83** *ag*- **8.69**	*g-g*-	*g*+*g*-	*ag*-	**4.78** *g-g*-
g+*a*	*aa*	*g-a*	*g*+*a*	*aa*	*g-a*	*g*+*a*	*aa*	*g-a*
7.80 *g*+*g*+ **7.61**	**4.61** *ag*+ **4.46**	**2.94** *g-g*+ **2.67**	**6.99** *g*+*g*+ **6.82**	**9.02** *ag*+ **8.68**	*g-g*+	*g*+*g*+	*ag*+	*g-g*+
g+*g*-	**7.93** *ag*- **7.63**	*g-g*-	**3.29** *g*+*g*- **3.02**	**0.81** *ag*- **0.73**	**4.27** *g-g*- **3.95**	*g*+*g*-	*ag*-	*g-g*-
g+*a*	*aa*	*g-a*	*g*+*a*	*aa*	*g-a*	*g*+*a*	*aa*	*g-a*
g+*g*+	**7.90** *ag*+ **7.69**	*g-g*+	**3.21** *g*+*g*+ **3.02**	**1.04** *ag*+ **0.75**	**4.22** *g-g*+ **3.97**	*g*+*g*+	*ag*+	*g-g*+
g+*g*-	**8.12** *ag*- **7.71**	**5.78** *g-g*- **5.44**	**2.10** *g*+*g*- **2.07**	*ag*-	*g-g*- **4.11**	**0.00** *g*+*g*- **0.00**	**1.06** *ag*- **0.81**	**1.48** *g-g*- **1.14**
g+*a*	*aa*	*g-a*	*g*+*a*	*aa*	*g-a*	*g*+*a*	*aa*	*g-a*
9.33 *g*+*g*+ **8.92**	**7.78** *ag*+ **7.71**	**5.79** *g-g*+ **5.44**	**2.33** *g*+*g*+ **2.07**	*ag*+	**4.25** *g-g*+ **4.11**	**0.31** *g*+*g*+ **0.00**	**0.87** *ag*+ **0.82**	**1.30** *g-g*+ **1.03**

Figure 12. Relative energies (kcal mol^{-1}) represented in a 4D-Ramachandran topological matrix, for N-acetyl-tyrosyl-N-methylamide (upper value) and N-acetyl-phenylalanyl-N-methylamide (lower value), computed at the B3LYP/6-31G(d) level of theory. The conformational assignments (middle) denote the χ_i^1 andχ_i^2 conformations, respectively.

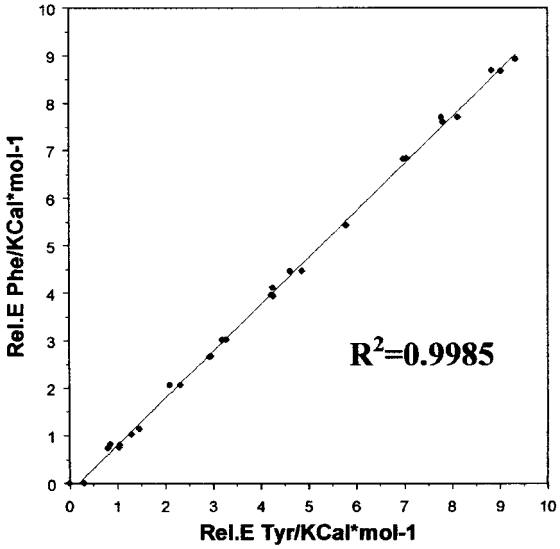

Figure 13. Linear fit plot of Rel.E_{Tyr} against Rel.E_{Phe}, for matching conformers, computed at the B3LYP/6-31G(d) level of theory.

3.2 Molecular energetics

Tables 2 and 3 present the total as well as the relative energy (ΔE) of Tyr and Phe diamides, respectively. The relative energies are included in a 4*D*-Ramachandran topological matrix in Figure 12, with relative energy comprising the 5th dimension. The differences between these two sets of ΔE values [$\Delta E = \Delta E_{\mathrm{Tyr}} - \Delta E_{\mathrm{Phe}}$] are also presented in Table 4. A linear correlation between ΔE_{Tyr} and ΔE_{Phe} is shown in Figure 13.

Figure 12 reveals that the $\gamma_{\mathrm{D}} g^+ g^-$ and $\alpha_{\mathrm{D}} g^+ g^-$ conformers were not found for the phenylalanyl system, but were stable minima for the tyrosyl system.

The $\delta_{\mathrm{L}} g^- g^-$ conformer for the phenylalanyl system may have been replaced by the $\alpha_{\mathrm{L}} g^- g^-$ conformer in the tyrosyl system.

3.3 Aromatic backbone interactions

The Ar–[HNCO(i)] and Ar–[HNCO(i+1)] distances found in Tables 5 and 6 show no significant difference between the Tyr and Phe residues. Interaction distances below 4.1 Å appear in bold with near exact trend preservation between the two sets. The differences in these distances, d[Tyr] − d[Phe] are listed in Table 7. A summary of the number of conformers for each interaction type is listed in Table 8. It is clear from Tables 7 and 8 that the same conformer set, number and type of interactions are found for the phenylalanyl and tyrosyl model systems.

Although slightly, the Ar–[HNC=O(i)] and Ar–[HNC=O(i+1)] distances for the phenylalanyl conformers are shorter than those for the matching tyrosyl conformers, regardless of the type of Ar interaction (Ar–HNC=O *vs.* Ar–O=CNH), apparnet in Table 7. These deviations in distance are not absolute (*i.e.* always shorter for one system) and mentioned only in qualitative observation, as there are a number of exceptions. A more detailed examination of the charge densities about each aromatic centroid of charge is necessary to quantify these distance trends. These are due primarily to the electrostatic nature [7] of the interactions, which do not always follow geometric trends. Specifically, the distance between two interacting points cannot be considered independently; factors such as molecular orbital symmetry also contribute to the strength of the Ar–[HNC=O(i)] and Ar–[HNC=O($i+1$)] interactions.

4 Conclusions

The results of MDCA of N-acetyl-tyrosyl-N-methylamide and N-acetyl-phenylalanyl-N-methyalmide suggest that the coupling of the *p*-OH group on the remainder of the peptide structure is indeed present, although much less pronounced geometrically than thought at the onset of this work. Perhaps a much larger differentiation than the one observed between the tyrosyl and phenylalanyl systems studied here exists in terms of the charge densities and their roles in the intramolecular interactions reported. Since the two systems are nearly identical, with the exception of the *p*-OH group in the side chain of tyrosyl, the "modular" nature of the molecular elements comprising

Table 5. Backbone-backbone H-bond and aromatic geometric centroid distances to all atoms of peptide groups (i) and ($i+1$), in angstroms for N-acetyl-phenylalanyl-N-methylamide computed at the B3LYP/6-31G(d) level of theory.

	Conformer				β_L*	Ar$\cdots$Y(i)/Å				$\gamma_{L/D}$**	Ar$\cdots$Y($i+1$)/Å			
Label	ϕ_1	ψ_1	χ_1	χ_1	H$\cdots$O	Y=H	Y=N	Y=C	Y=O	H$\cdots$O	Y=H	Y=N	Y=C	Y=O
	a	a	g^+	g^+	2.142	**4.091**	4.064	4.898	5.369	4.976	5.101	4.799	4.119	4.254
	a	a	g^+	a										
	a	a	g^+	g^-	2.140	**4.091**	4.062	4.917	5.397	4.975	5.107	4.789	4.121	4.266
	a	a	a	g^+	2.115	5.872	5.120	5.590	5.087	5.017	**3.045**	3.966	4.437	5.623
β_L	a	a	a	a										
	a	a	a	g^-	2.115	5.872	5.121	5.593	5.092	5.008	**3.046**	3.959	4.435	5.621
	a	a	g^-	g^+	2.336	4.709	4.030	4.261	4.175	4.384	5.680	5.937	5.240	5.906
	a	a	g^-	a										
	a	a	g^-	g^-	2.349	4.700	4.032	4.267	4.184	4.369	5.691	5.942	5.240	5.902
	g^-	g^+	g^+	g^+	3.847	**3.052**	3.818	5.082	6.090	1.963	5.965	5.637	4.485	4.365
	g^-	g^+	g^+	a										
	g^-	g^+	g^+	g^-	3.846	**3.052**	3.817	5.081	6.090	1.964	5.969	5.639	4.487	4.366
	g^-	g^+	a	g^+	3.525	5.498	5.139	6.143	6.207	2.074	5.435	5.112	4.262	4.360
γ_L	g^-	g^+	a	a										
	g^-	g^+	a	g^-	3.504	5.505	5.138	6.145	6.205	2.076	5.428	5.113	4.264	4.366
	g^-	g^+	g^-	g^+	3.739	**3.616**	3.907	4.743	5.442	2.000	6.107	6.237	5.264	5.692
	g^-	g^+	g^-	a										
	g^-	g^+	g^-	g^-	3.741	**3.599**	3.904	4.752	5.463	1.997	6.126	6.242	5.263	5.696
	g^+	g^-	g^+	g^+	4.300	5.027	4.281	4.164	**3.713**	1.799	**3.996**	4.348	4.192	4.815
	g^+	g^-	g^+	a										
	g^+	g^-	g^+	g^-										
	g^+	g^-	a	g^+	3.626	5.723	5.160	5.965	5.828	2.077	4.943	4.640	4.077	4.329
γ_D	g^+	g^-	a	a										
	g^+	g^-	a	g^-	3.777	5.764	5.187	5.980	5.835	1.940	4.979	4.649	4.062	4.270
	g^+	g^-	g^-	g^+	4.002	**4.079**	**3.977**	4.431	4.824	1.920	5.647	5.950	5.248	5.915
	g^+	g^-	g^-	a										
	g^+	g^-	g^-	g^-	4.000	**4.079**	**3.977**	4.429	4.821	1.920	5.644	5.948	5.248	5.917
	a	g^+	g^+	g^+	4.034	**3.265**	3.939	5.144	6.047	3.494	5.016	4.890	4.231	4.500
	a	g^+	g^+	a										
	a	g^+	g^+	g^-	4.033	**3.264**	3.939	5.142	6.046	3.492	5.021	4.894	4.232	4.499
	a	g^+	a	g^+										
δ_L	a	g^+	a	a										
	a	g^+	a	g^-										
	a	g^+	g^-	g^+	4.084	**4.044**	3.991	4.204	4.480	3.459	6.115	6.228	5.241	5.661
	a	g^+	g^-	a										
	a	g^+	g^-	g^-	4.086	**4.035**	3.990	4.203	4.485	3.458	6.113	6.227	5.242	5.662
	a	g^-	g^+	g^+	3.600	4.597	4.093	4.656	4.795	4.560	**3.264**	3.949	4.152	5.018
	a	g^-	g^+	a										
	a	g^-	g^+	g^-	3.594	4.588	4.090	4.638	4.781	4.557	**3.255**	3.949	4.166	5.046
	a	g^-	a	g^+	3.463	5.875	5.181	5.836	5.485	4.785	4.951	4.853	4.094	4.221
δ_D	a	g^-	a	a										
	a	g^-	a	g^-	3.463	5.875	5.182	5.840	5.492	4.790	4.944	4.850	4.089	4.212
	a	g^-	g^-	g^+										
	a	g^-	g^-	a										
	a	g^-	g^-	g^-										
	g^-	g^-	g^+	g^+										
	g^-	g^-	g^+	a										
	g^-	g^-	g^+	g^-										
	g^-	g^-	a	g^+										
α_L	g^-	g^-	a	a										
	g^-	g^-	a	g^-										
	g^-	g^-	g^-	g^+										
	g^-	g^-	g^-	a										
	g^-	g^-	g^-	g^-										
	g^+	g^+	g^+	g^+	4.448	4.414	4.010	3.756	**3.645**	2.774	5.699	5.565	4.476	4.477
	g^+	g^+	g^+	a										
	g^+	g^+	g^+	g^-										
	g^+	g^+	a	g^+	4.436	5.174	5.011	5.934	6.076	3.116	6.206	5.834	4.612	4.440
α_D	g^+	g^+	a	a										
	g^+	g^+	a	g^-	4.436	5.170	5.008	5.931	6.075	3.112	6.211	5.839	4.616	4.444
	g^+	g^+	g^-	g^+	4.419	**3.811**	**3.969**	4.434	4.904	2.989	6.117	6.234	5.239	5.657
	g^+	g^+	g^-	a										
	g^+	g^+	g^-	g^-	4.424	**3.788**	**3.967**	4.453	4.973	2.976	6.120	6.233	5.239	5.661
	g^-	a	g^+	g^+										
	g^-	a	g^+	a										
	g^-	a	g^+	g^-										
	g^-a	a	g^+											
ε_L	g^-	a	a	a										
	g^-	a	a	g^-										
	g^-	a	g^-	g^+										
	g^-	a	g^-	a										
	g^-	a	g^-	g^-										
	g^+	a	g^+	g^+										
	g^+	a	g^+	a										
	g^+	a	g^+	g^-										
	g^+	a	a	g^+	2.753	5.808	5.178	5.996	5.799	4.364	**2.953**	3.903	4.439	5.656
ε_D	g^+	a	a	a										
	g^+	a	a	g^-	2.741	5.808	5.176	5.995	5.799	4.338	**2.958**	3.910	4.454	5.671
	g^+	a	g^-	g^+										
	g^+	a	g^-	a										
	g^+	a	g^-	g^-										

* β_L conformers form a O(i)$\cdots$HN(i) BB-BB H-bonds, referred to as C_5. ** $\gamma_{L/D}$ conformers form O($i-1$)$\cdots$HN($i+1$) BB-BB H-bonds, referred to as C_7.

Table 6. Backbone-backbone H-bond and aromatic geometric centroid distances to all atoms of peptide groups (i) and ($i+1$), in angstroms for N-acetyl-phenylalanyl-N-methylamide computed at the B3LYP/6-31G(d) level of theory.

	Conformer				β_L*	Ar$\cdots$Y(i)/Å				$\gamma_{L/D}$**	Ar$\cdots$Y($i+1$)/Å			
Label	ϕ_1	ψ_1	χ_1	χ_1	H$\cdots$O	Y=H	Y=N	Y=C	Y=O	H$\cdots$O	Y=H	Y=N	Y=C	Y=O
	a	a	g^+	g^+	2.144	**4.075**	4.065	4.910	5.403	4.977	5.074	4.788	4.118	4.263
	a	a	g^+	a										
	a	a	g^+	g^-	2.156	**4.046**	4.055	4.928	5.436	4.951	5.111	4.808	4.115	4.236
	a	a	a	g^+	2.117	**5.876**	5.138	5.631	5.148	5.008	**3.031**	3.940	4.418	5.594
β_L	a	a	a	a										
	a	a	a	g^-	2.114	**5.878**	5.123	5.588	5.081	5.011	**3.062**	3.978	4.450	5.636
	a	a	g^-	g^+	2.315	**4.664**	3.985	4.152	**4.064**	4.485	5.708	5.946	5.246	5.911
	a	a	g^-	a										
	a	a	g^-	g^-	2.353	4.732	4.069	4.385	4.337	4.313	5.672	5.934	5.247	5.920
	g^-	g^+	g^+	g^+	3.874	**3.070**	3.833	5.098	6.105	1.955	5.956	5.603	4.473	4.368
	g^-	g^+	g^+	a										
	g^-	g^+	g^+	g^-	3.871	**3.070**	3.833	5.098	6.104	1.955	5.950	5.599	4.467	4.357
	g^-	g^+	a	g^+	3.514	5.507	5.149	6.162	6.229	2.068	5.149	5.126	4.265	4.352
γ_L	g^-	g^+	a	a										
	g^-	g^+	a	g^-	3.496	5.513	5.150	6.163	6.227	2.078	5.442	5.121	4.265	4.356
	g^-	g^+	g^-	g^+	3.752	**3.594**	3.914	4.751	5.460	1.997	6.117	6.246	5.270	5.696
	g^-	g^+	g^-	a										
	g^-	g^+	g^-	g^-	3.758	**3.552**	3.904	4.750	5.480	1.996	6.140	6.254	5.271	5.697
	g^+	g^-	g^+	g^+	4.283	5.085	4.310	4.209	3.723	1.802	**3.953**	4.310	4.180	4.809
	g^+	g^-	g^+	a										
	g^+	g^-	g^+	g^-	4.306	5.022	4.281	4.162	3.712	1.797	4.018	4.381	4.204	4.815
	g^+	g^-	a	g^+	3.778	5.766	5.192	5.987	5.847	1.937	4.992	4.662	4.070	4.274
γ_D	g^+	g^-	a	a										
	g^+	g^-	a	g^-	3.746	5.794	5.197	5.989	5.831	1.964	4.856	4.550	4.031	4.284
	g^+	g^-	g^-	g^+	3.999	**4.084**	3.980	4.435	4.827	1.921	5.650	5.953	5.255	5.925
	g^+	g^-	g^-	a										
	g^+	g^-	g^-	g^-	3.982	**4.094**	3.980	4.420	4.802	1.924	5.632	5.940	5.258	5.944
	a	g^+	g^+	g^+	4.018	**3.282**	3.956	5.151	6.053	3.484	5.074	4.932	4.250	4.497
	a	g^+	g^+	a										
	a	g^+	g^+	g^-	4.016	**3.288**	3.959	5.155	6.055	3.489	5.065	4.920	4.237	4.478
	a	g^+	a	g^+										
δ_L	a	g^+	a	a										
	a	g^+	a	g^-										
	a	g^+	g^-	g^+	4.087	**4.025**	3.984	4.179	4.462	3.482	6.108	6.227	5.247	5.674
	a	g^+	g^-	a										
	ag^+	g^-	g^-											
	a	g^-	g^+	g^+	3.580	4.550	4.075	4.643	4.816	4.590	**3.232**	**3.955**	4.196	5.102
	a	g^-	g^+											
	a	g^-	g^+	g^-	3.604	4.590	4.099	4.676	4.841	4.565	**3.253**	**3.936**	4.152	5.019
	a	g^-	a	g^+	3.470	5.886	5.186	5.833	5.475	4.776	4.998	4.892	4.107	4.212
δ_D	a	g^-	a	a										
	a	g^-	a	g^-	3.452	5.868	5.189	5.862	5.529	4.819	4.853	4.795	4.082	4.251
	a	g^-	g^-	g^+										
	a	g^-	g^-	a										
	a	g^-	g^-	g^-										
	g^-	g^-	g^+	g^+										
	g^-	g^-	g^+	a										
	g^-	g^-	g^+	g^-										
	g^-	g^-	a	g^+										
α_L	g^-	g^-	a	a										
	g^-	g^-	a	g^-										
	g^-	g^-	g^-	g^+										
	g^-	g^-	g^-	a										
	g^-	g^-	g^-	g^-	4.380	**3.435**	3.959	4.832	5.573	3.063	5.952	6.107	5.245	5.749
	g^+	g^+	g^+	g^+	4.447	4.437	4.035	3.780	**3.675**	2.755	5.699	5.565	4.473	4.465
	g^+	g^+	g^+	a										
	g^+	g^+	g^+	g^-										
	g^+	g^+	a	g^+	4.438	5.251	5.061	5.983	6.103	3.126	6.173	5.773	4.558	4.362
α_D	g^+	g^+	a	a										
	g^+	g^+	a	g^-	4.436	5.206	5.031	5.954	6.087	3.107	6.219	5.831	4.607	4.426
	g^+	g^+	g^-	g^+	4.447	**3.813**	3.976	4.440	4.912	2.755	6.125	6.242	5.247	5.666
	g^+	g^+	g^-	a										
	g^+	g^+	g^-	g^-	4.418	**3.807**	3.966	4.407	4.874	2.989	6.119	6.240	5.249	5.672
	g^-	a	g^+	g^+										
	g^-	a	g^+	a										
	g^-	a	g^+	g^-										
	g^-	a	a	g^+										
ε_L	g^-	a	a	a										
	g^-	a	a	g^-										
	g^-a	g^-	g^+											
	g^-	ag^-	a											
	g^-	a	g^-	g^-										
	g^+	a	g^+	g^+										
	g^+	a	g^+	a										
	g^+	a	g^+	g^-										
	g^+	a	a	g^+	2.759	5.823	5.190	6.004	5.804	4.359	**2.946**	3.901	4.444	5.662
ε_D	g^+	a	a	a										
	g^+	a	a	g^-	2.739	5.820	5.186	6.001	5.802	4.338	**2.951**	3.907	4.457	5.674
	g^+	a	g^-	g^+										
	g^+	a	g^-	a										
	g^+		g^-	g^-										

* β_L conformers form a O(i)$\cdots$HN(i) BB-BB H-bonds, referred to as C_5. ** $\gamma_{L/D}$ conformers form O($i-1$)$\cdots$HN($i+1$) BB-BB H-bonds, referred to as C_7.

Table 7. Backbone-backbone H-bond and aromatic geometric centroid distances to all atoms of peptide groups (i) and (i+1), in angstroms for [Ac-Tyr-NH-Me] − [Ac-Phe-NH-Me], for matching conformers computed at the B3LYP/6-31G(d) level of theory.

	Conformer				β_L*	Ar$\cdots$Y(i)/Å				$\gamma_{L/D}$**	Ar$\cdots$Y($i+1$)/Å			
Label	ϕ_1	ψ_1	χ_1	χ_1	H$\cdots$O	Y=H	Y=N	Y=C	Y=O	H$\cdots$O	Y=H	Y=N	Y=C	Y=O
	a	a	g^+	g^+	0.002	−0.016	0.001	0.012	0.034	0.001	−0.027	−0.011	−0.001	0.009
	a	a	g^+	a										
	a	a	g^+	g^-	0.016	−0.045	−0.007	0.011	0.039	−0.024	0.004	0.019	−0.006	−0.030
	a	a	a	g^+	0.002	0.004	0.018	0.041	0.061	−0.009	−0.014	−0.026	−0.019	−0.029
β_L	a	a	a	a										
	a	a	a	g^-	−0.001	0.006	0.002	−0.005	−0.011	0.003	0.016	0.019	0.015	0.015
	a	a	g^-	g^+	−0.021	−0.045	−0.045	−0.109	−0.111	0.101	0.028	0.009	0.006	0.005
	a	a	g^-	a										
	a	a	g^-	g^-	0.004	0.032	0.037	0.118	0.153	−0.056	−0.019	−0.008	0.007	0.018
	g^-	g^+	g^+	g^+	0.027	0.018	0.015	0.016	0.015	−0.008	−0.009	−0.034	−0.012	0.003
	g^-	g^+	g^+	a										
	g^-	g^+	g^+	g^-	0.025	0.018	0.016	0.017	0.014	−0.009	−0.019	−0.040	−0.020	−0.009
	g^-	g^+	a	g^+	−0.011	0.009	0.010	0.019	0.022	−0.006	−0.286	0.014	0.003	−0.008
γ_L	g^-	g^+	a	a										
	g^-	g^+	a	g^-	−0.008	0.008	0.012	0.018	0.022	0.002	0.014	0.008	0.001	−0.010
	g^-	g^+	g^-	g^+	0.013	−0.022	0.007	0.008	0.018	−0.003	0.010	0.009	0.006	0.004
	g^-	g^+	g^-	a										
	g^-	g^+	g^-	g^-	0.017	−0.047	0.000	−0.002	0.017	−0.001	0.014	0.012	0.008	0.001
	g^+	g^-	g^+	g^+	−0.017	0.058	0.029	0.045	0.010	0.003	−0.043	−0.038	−0.012	−0.006
	g^+	g^-	g^+	a										
	g^+	g^-	g^+	g^-										
	g^+	g^-	a	g^+	0.152	0.043	0.032	0.022	0.019	−0.140	0.049	0.022	−0.007	−0.055
γ_D	g^+	g^-	a	a										
	g^+	g^-	a	g^-	−0.031	0.030	0.010	0.009	−0.004	0.024	−0.123	−0.099	−0.031	0.014
	g^+	g^-	g^-	g^+	−0.003	0.005	0.003	0.004	0.003	0.001	0.003	0.003	0.007	0.010
	g^+	g^-	g^-	a										
	g^+	g^-	g^-	g^-	−0.018	0.015	0.003	−0.009	−0.019	0.004	−0.012	−0.008	0.010	0.027
	a	g^+	g^+	g^+	−0.016	0.017	0.017	0.007	0.006	−0.010	0.058	0.042	0.019	−0.003
	a	g^+	g^+	a										
	a	g^+	g^+	g^-	−0.017	0.024	0.02	0.013	0.009	−0.003	0.044	0.026	0.005	−0.021
	a	g^+	a	g^+										
δ_L	a	g^+	a	a										
	a	g^+	a	g^-										
	a	g^+	g^-	g^+	0.003	−0.019	−0.007	−0.025	−0.018	0.023	−0.007	−0.001	0.006	0.013
	a	g^+	g^-	a										
	a	g^+	g^-	g^-										
	a	g^-	g^+	g^+	−0.020	−0.047	−0.018	−0.013	0.021	0.030	−0.032	0.006	0.044	0.084
	a	g^-	g^+	a										
	a	g^-	g^+	g^-	0.010	0.002	0.009	0.038	0.060	0.008	−0.002	−0.013	−0.014	−0.027
	a	g^-	a	g^+	0.007	0.011	0.005	−0.003	−0.010	−0.009	0.047	0.039	0.013	−0.009
δ_D	a	g^-	a	a										
	a	g^-	a	g^-	−0.011	−0.007	0.007	0.022	0.037	0.029	−0.091	−0.055	−0.007	0.039
	a	g^-	g^-	g^+										
	a	g^-	g^-	a										
	a	g^-	g^-	g^-										
	g^-	g^-	g^+	g^+										
	g^-	g^-	g^+	a										
	g^-	g^-	g^+	g^-										
	g^-	g^-	a	g^+										
α_L	g^-	g^-	a	a										
	g^-	g^-	a	g^-										
	g^-	g^-	g^-	g^+										
	g^-	g^-	g^-	a										
	g^-	g^-	g^-	g^-										
	g^+	g^+	g^+	g^+	−0.001	0.023	0.025	0.024	0.030	−0.019	0.000	0.000	−0.003	−0.012
	g^+	g^+	g^+	a										
	g^+	g^+	g^+	g^-										
	g^+	g^+	a	g^+	0.002	0.077	0.050	0.049	0.027	0.010	−0.033	−0.061	−0.054	−0.078
α_D	g^+	g^+	a	a										
	g^+	g^+	a	g^-	0.000	0.036	0.023	0.023	0.012	−0.005	0.008	−0.008	−0.009	−0.018
	g^+	g^+	g^-	g^+	0.028	0.002	0.007	0.006	0.008	−0.234	0.008	0.008	0.008	0.009
	g^+	g^+	g^-	a										
	g^+	g^+	g^-	g^-	−0.006	0.019	−0.001	−0.046	−0.099	0.013	−0.001	0.007	0.010	0.011
	g^-	a	g^+	g^+										
	g^-	a	g^+	a										
	g^-	a	g^+	g^-										
	g^-	a	a	g^+										
ε_L	g^-	a	a	a										
	g^-	a	a	g^-										
	g^-	a	g^-	g^+										
	g^-	a	g^-	a										
	g^-	a	g^-	g^-										
	g^+	a	g^+	g^+										
	g^+	a	g^+	a										
	g^+	a	g^+	g^-										
	g^+	a	a	g^+	0.006	0.015	0.012	0.008	0.005	−0.005	−0.007	−0.002	0.005	0.006
ε_D	g^+	a	a	a										
	g^+	a	a	g^-	−0.002	0.012	0.010	0.006	0.003	0.000	−0.007	−0.003	0.003	0.003
	g^+	a	g^-	g^+										
	g^+	a	g^-	a										
	g^+	a	g^-	g^-										

* β_L conformers form a O(i)$\cdots$HN(i) BB-BB H-bonds, referred to as C_5. ** $\gamma_{L/D}$ conformers, form O($i-1$)$\cdots$HN($i+1$) BB-BB H-bonds, referred to as C_7.

Table 8. Number of conformers with aromatic geometric centroid distances to selected atoms of peptide groups (i) and ($i+1$) ($i+1$) $\leq$ 4.1 Å for [Ac-Tyr-NH-Me] − [Ac-Phe-NH-Me], for matching conformers computed at the B3LYP/6-31G(d) level of theory.

	Position (i)		Position ($i+1$)	
System	amidic-H	carbonyl-O	amidic-H	carbonyl-O
phenylalanyl	14	2	7	0
tyrosyl	14	2	7	0

these systems is apparent. These "modules" include the peptide groups i and $i+1$, the tetrahedral-C_α, N- and C-terminal CH_3 groups, the H_2C_β-"spacer" and the aromatic rings. Each "module" is only slightly perturbed by the addition of the p-OH group. The magnitude of this perturbation on each "module" being inversely proportional to the distance from the added p-OH group and is clearly more of a field effect rather than an inductive one.

From the number of Ar–[HNCO(i, $i+1$)] interactions found for all stable conformers at the B3LYP/6-31G(d) level of theory it is evident that the p-OH substituent plays no role in the geometric requirements for these types of weak stabilizing forces. The strength of these interactions was not quantified nor compared between the two systems and it is still not clear what the difference is between these two residues. Nevertheless, the near identical sets of conformers and their respective geometries may indicate that the exact nature of the interactions was observed. The definition of the interaction used here is not quantitative, whereby the minimal distance defining such interactions is also non-standardized as yet. As reported, many conformers must be examined in depth to separate those that have actual electrostatic interactions and those that merely have the aromatic group by coincidence, within the Ar–[HNCO(i, $i+1$)] distance threshold used (4.1 Å).

Of course the full methodology could be repeated on any size peptide system within the limitations of computational power. It is predicted that the modular approach would allow for an automation of the conformational searches and data-extractions. Efficient scripting and coding could bring about the automation of tabulation and trend-recognition, within the standardized numerical definition of the systems so constructed. It is therefore quite easily envisaged that an n-dimensional structure activity relationship (n-D QSAR) is now possible using the numerical descriptions of model peptide systems outlined in this work.

This work was supported by grants from the NSF (EPS-0091900), NIH BRIN Program of the National Center for Research Resources (1 P20 RR16469) and Velocet Communications Inc., Toronto, Ontario, Canada. The authors thank Michelle A. Sahai, Jacqueline M.S. Law, Christopher N.J. Marai and Tania A. Pecora for helpful discussions, and preparation of tables and figures and Graydon Hoare for database management, network support and software and distributive processing development. A special thanks is extended to Andrew M. Chasse for his development of novel scripting and coding techniques which facilitate a reduction in the number of CPU cycles needed. The pioneering advances of Kenneth P. Chasse, in all composite computer-cluster software and hardware architectures, are also acknowledged. David C.L. Gilbert and Adam A. Heaney are also thanked for CPU time.

References

1. L.P. Hammett, J. Am. Chem. Soc. **59**, 96 (1937)
2. F. Ruff, I.G. Csizmadia, *Organic Reactions; Equilibria, Kinetics and Mechanism* (Elsevier, Amsterdam, 1994)
3. H.H. Jaffe, Chem. Rev. **53**, 191 (1953)
4. L.C. Snoek, E.G. Robertson, R.T. Kroemer, J.P. Simons, Chem. Phys. Lett. **321**, 49 (2000)
5. A. Perczel, J.G. Angyan, M. Kajtar, W. Viviani, J.L. Rivail, J.F. Marcoccia, I.G. Csizmadia, J. Am. Chem. Soc. **113**, 6256 (1991)
6. G. Tóth, R.F. Murphy, S. Lovas, Prot. Eng. **14**, 543 (2001)
7. C. Chipot, B. Maigret, D.A. Pearlman, P.A. Kollman, J. Am. Chem. Soc. **118**, 2998 (1996)
8. C. Chipot, R. Jaffe, B. Maigret, D.A. Pearlman, P.A. Kollman, J. Am. Chem. Soc. **118**, 11217 (1996)
9. G.B. McGaughey, M. Gagn, A.K. Rapp, J. Biol. Chem. **273**, 15458 (1998)
10. G. Duan, V.H. Smith Jr, D.F. Weaver, Chem. Phys. Lett. **310**, 323 (1999)
11. S. Tsuzuki, K. Honda, T. Uchimaru, M. Mikami, K. Tanabe, J. Am. Chem. Soc. **122**, 3746 (2000)
12. P. Tarakeshwar, H.S. Choi, K.S. Kim, J. Am. Chem. Soc. **123**, 3323 (2001)
13. T. Steiner, Act. Cryst. D **54**, 584 (1998)
14. G. Tóth, C.R. Watts, R.F. Murphy, S. Lovas, Proteins **43**, 373 (2001)
15. G. Tóth, R.F. Murphy, S. Lovas, J. Am. Chem. Soc. **123**, 11782 (2001)
16. T. Steiner, G. Koellner, J. Mol. Biol. **305**, 535 (2001)
17. E. Langella, N. Rega, R. Improta, O. Crescenzi, V. Barone, J. Comput. Chem. **23**, 650 (2002)
18. G. Chass, M.A. Sahai, J.M.S. Law, S. Lovas, Ö. Farkas, A. Perczel, J.L. Rivail, I.G. Csizmadia, Int. J. Quant. Chem. **90**, issue 2 (2002)
19. Arch. Biochem. Biosphys. **145**, 405 (1971)
20. Biochem. J. **121**, 577 (1971)
21. Biochemistry. J. **9**, 3471 (1971)
22. Biochim. Biophys. Acta. **229**, 1 (1971)
23. Eur. J. Biochem. **17**, 193 (1969)
24. J. Biol. Chem. **245**, 6489 (1970)
25. J. Mol. Biol. **52**, 1 (1970)
26. Pure Appl. Chem. **40**, 291 (1974)
27. *Bio Biochemical Nomenclature and Related Documents*, 2nd edn. (Portland Press, 1992), pp. 73-81
28. *Gaussian 98*, Revision A.11, M.J. Frisch, G.W. Trucks, H.B. Schlegel, G.E. Scuseria, M.A. Robb, J.R. Cheeseman, V.G. Zakrzewski, J.A. Montgomery Jr., R.E. Stratmann,

J.C. Burant, S. Dapprich, J.M. Millam, A.D. Daniels, K.N. Kudin, M.C. Strain, Ö. Farkas, J. Tomasi, V. Barone, M. Cossi, R. Cammi, B. Mennucci, C. Pomelli, C. Adamo, S. Clifford, J. Ochterski, G.A. Petersson, P.Y. Ayala, Q. Cui, K. Morokuma, P. Salvador, J.J. Dannenberg, D.K. Malick, A.D. Rabuck, K. Raghavachari, J.B. Foresman, J. Cioslowski, J.V. Ortiz, A.G. Baboul, B.B. Stefanov, G. Liu, A. Liashenko, P. Piskorz, I. Komaromi, R. Gomperts, R.L. Martin, D.J. Fox, T. Keith, M.A. Al-Laham, C.Y. Peng, A. Nanayakkara, M. Challacombe, P.M.W. Gill, B. Johnson, W. Chen, M.W. Wong, J.L. Andres, C. Gonzalez, M. Head-Gordon, E.S. Replogle, J.A. Pople, Gaussian, Inc., Pittsburgh PA, 2001

29. A. Perczel, R. Daudel, J.G. Angyan, I.G. Csizmadia, Can. J. Chem. **68**, 1882 (1990)
30. A. Perczel, J.G. Angyan, M. Kajtar, W. Viviani, J.L. Rivail, J.F. Marcoccia, I.G. Csizmadia, J. Am. Chem. Soc. **113**, 6256 (1991)
31. M.A. McAllister, A.Perczel, P. Császár, I.G. Csizmadia, J. Mol. Struct. (Theochem) **288**, 181 (1993)
32. A. Perczel, M.A. McAllister, P. Császár, I.G. Csizmadia, J. Am. Chem. Soc. **115**, 4849 (1993)
33. A. Perczel, M.A. McAllister, P. Császár, I.G. Csizmadia, Can. J. Chem. **72**, 2050 (1994)
34. M. Cheung, M.E. McGovern, T. Jin, D.C. Zhao, M.A. McAllister, A. Perczel, P. Császár, I.G. Csizmadia, J. Mol. Struct. (Theochem) **309**, 151 (1994)
35. Ö. Farkas, S.J. Salpietro, P. Császár, I.G. Csizmadia , J. mol. Struct. (Theochem) **367**, 25 (1996)